Published in final edited form as:
*Epigenetics*. 2008 ; 3(4): 216–229.

# Maize lines expressing RNAi to chromatin remodeling factors are similarly hypersensitive to UV-B radiation but exhibit distinct transcriptome responses

**Paula Casati**[1,*] and **Virginia Walbot**[2]

1*Centro de Estudios Fotosintéticos y Bioquímicos (CEFOBI), Facultad de Ciencias Bioquímicas y Farmacéuticas, Universidad Nacional de Rosario, Suipacha 531, 2000 Rosario, Argentina*

2*Department of Biology, 385 Serra Mall, Stanford University, Stanford, CA, USA 94305−5020. walbot@stanford.edu*

## Abstract

RNAi knockdown lines targeting two putative chromatin factors (a methyl-CpG-binding domain protein MBD101 and a chromatin remodeling complex protein CHC101) exhibit identical phenotypic consequences after UV-B exposure including necrosis in adult leaves and seedling death. Here we report that these RNAi lines exhibit substantially different transcriptome changes assessed on a 44K Agilent oligonucleotide array platform compared to each other and to UV-B tolerant non-transgenic siblings both before and after 8 h of UV-B exposure. Adult maize leaves express ~26,000 transcript types under greenhouse growth conditions; after 8 h of UV-B exposure 267 transcripts exhibit an expression change in the B73 control line. Most of these transcript abundance changes in B73 after UV-B treatment are not found in the two RNAi knockdown lines: 119 up-regulated transcript types and 128 down-regulated types are uniquely modulated in B73. The *mbd101* RNAi line shows many more line-specific transcript changes (897 up, 68 down) than either B73 or the *chc101*line (72 up, 103 down). By functional analysis, the largest category of genes with predicted functions affected by UV-B is the DNA/chromatin binding group. Differential activation of suites of transcription factors in the control and transgenic lines are the likely explanation for the divergent transcriptome profiles.

### Keywords

ultraviolet-B; Zea mays; microarrays; transcriptome; transcription factors

## Introduction

Genetic information encoded by eukaryotic DNA is compacted into chromatin permitting the genome to fit within the nucleus (for a review, see ref. 1). The basic unit of chromatin is the nucleosome, which is formed by wrapping 147 bp of DNA around a histone octamer; the nucleosomal structure is a barrier to proteins that act by contacting DNA including most transcription factors and the general transcriptional machinery. Gene expression required to maintain a normal phenotype is regulated by altering chromatin structure in response to various stimuli. 1-3 This chromatin restructuring is accomplished by three distinct processes that collectively regulate gene expression. First covalent modification of histone amino acids

*Correspondence to: Paula Casati, Centro de Estudios Fotosintéticos y Bioquímicos (CEFOBI), Facultad de Ciencias Bioquímicas y Farmacéuticas, Universidad Nacional de Rosario, Suipacha 531, 2000 Rosario, Argentina; E-mail: casati@cefobi.gov.ar..

primarily in the N-terminal tails is accomplished by suites of histone modifying enzymes, changing histone–DNA interaction and thus changing protein binding affinities. Second, chromatin remodeling complexes alter histone–DNA interaction, facilitating nucleosome sliding to a new position, conformational changes in histone–DNA interactions, and histone loss or nucleosome disassembly. Third, methylation of DNA cytosine residues obstructs binding of some proteins and recruits others, including transcription factors. 1-3

Sessile plants are constantly exposed to diverse environmental perturbations and to survive they must acclimate to abiotic conditions such as excessive or inadequate light, water, salt, temperature, and pathogens. Because plants capture light for photosynthesis they also experience fluctuating solar ultraviolet-B radiation (UV-B 290−320 nm), and this energetic radiation causes direct damage to DNA, proteins, lipids, and RNA. 4-6 Plant acclimation responses include repair 7,8 and avoidance. 9,10 The mechanisms plants use for sensing and responding to UV-B have not been identified, 11-13 but some components in the UVB-induced signal transduction cascade have been identified recently in *Arabidopsis thaliana*. The bZIP transcription factor HY5 is required in both UV-B and for growth in visible light. 14 UVR8 is a UV-B specific factor with sequence similarity to the eukaryotic guanine nucleotide exchange factor RCC1. UVR8 is located principally in the nucleus and associates with chromatin via histones. 15

In maize, chromatin remodeling has also been implicated in UV-B responses, a discovery from transcriptome profiling of lines differing in UV-B sensitivity. Because there is less air mass and greater atmospheric transparency to shorter wavelengths, plants at high altitudes generally experience higher UV-B radiation flux. 16 We previously reported that maize landraces from high altitudes have adaptations (specific alleles) that increase UV-B tolerance; 17 they constitutively express higher levels of genes predicted to encode chromatin remodeling factors than temperate zone lines and then acclimate by showing greater UV-B mediated up-regulation of these genes. 18 To test the hypothesis that chromatin remodeling capacity is essential, transgenic plants (in the temperate B73 inbred) expressing RNAi to reduce four chromatin factors were found to be acutely sensitive to UV-B at doses that do not cause visible damage to maize lacking flavonoid sunscreens. Symptoms included necrotic sun burning of adult tissue, decreased photosynthetic pigments, altered expression of some UV-B-regulated genes, and seedling lethality. 18 These RNAi-expressing lines showed no symptoms in visible light and control, non-transgenic siblings in a UV-B tolerant temperate zone line (B73) lacked symptoms in UV-B. At the chromatin level, mass spectromic analysis of post-translational histone modifications demonstrated that UV-B tolerant B73 and high altitude landraces exhibit greater acetylation of N-terminal H3 and H4 tails after irradiation19 than UV-B sensitive temperate (W23 background) and the RNAi knockdown lines. These acetylated histones are enriched in the promoters and transcribed regions of UV-B up-regulated genes. 19 Therefore, chromatin remodeling capacity is important for effective responses to UV-B and loss of capacity is associated with hypersensitivity.

Two of the RNAi lines used in the previous study were knockdown for *chc101* and *mbd101* genes. *chc101* encodes a putative component of the SWItch/Sucrose NonFermenting (SWI/SNF) and Remodel the Structure of Chromatin (RSC) chromatin remodeling complex; CHC101 is a SWIB domain-containing protein and is a likely homolog of yeast Swp73 and Rsc6 proteins and human SMARD proteins. *mbd101* encodes a putative methyl-CpG-binding domain (MBD) protein. Even though the precise roles of CHC101 and MBD101 have not been demonstrated in maize, the compelling biology is that both *chc101* and *mbd101* knockdown plants are hypersensitive to UV-B. 18 In this work, the transcriptome consequences of reduced expression of *chc101* and *mbd101* were analyzed under control greenhouse conditions and after 8 h UV-B with reference to non-transgenic B73 siblings. The *mbd101* and *chc101* RNAi lines have very distinctive differences to B73 controls and to each other in the standard growth

conditions and after supplementary radiation treatment. The largest number of differentially regulated genes in all comparisons is the DNA/chromatin binding category in both control light and after UV-B. We discuss how the alterations in steady-state normal gene expression and altered responses to UV-B in the RNAi knockdowns can be distinctive and nonetheless both result in acute hypersensitivity to UV-B radiation.

## Results

### Biological materials, microarray design and data analysis

A primary goal in this work was to investigate if increased sensitivity to UV-B radiation by transgenic plants showing decreased transcript levels of two putative chromatin proteins, MBD101 and CHC101, reflects inappropriate transcriptional regulation of acclimation genes. Prior work had demonstrated that both lines express lower levels of several chromatin factors, thus a second goal was to determine to what extent the transcriptomes of these lines overlap, both before and after UV-B treatment. 18 To address these points, we initiated a genomic scale analysis by performing expression-profiling experiments using 44K Agilent arrays containing 60-mer *in situ* synthesized oligo probes; probe sets are provided in quadruplicate in an array of 4×44, which allowed four pairs of independent hybridizations to be done on one slide. Prior microarray profiling of maize leaf gene expression utilized platforms available at that time, each with a major limitation. Initial work with spotted ESTs20,21 provided limited coverage of the expected ~50,000 maize genes and could not distinguish hybridization among gene family members. The Affymetrix maize chip has features for detecting approximately 12,000 genes and the 25-mer probe sets work well with the maize inbred lines utilized in probe design and less well with other lines and landraces given the high allelic diversity in maize. 22 An Agilent 22K *in situ* synthesized 60-mer array yielded high quality data for 11K sense and 11K matched antisense probes, and extended but still limited gene coverage.23 A platform with spotted 70-mer oligonucleotide probes capable of detecting about 40,000 maize genes provided good coverage but yielded inconsistent data, 24 because of a high frequency of malformed spots. 25 A new Agilent array type printed with 44K features in four grids on one slide provides coverage for approximately 39,000 maize genes and can thus refine and extend knowledge about maize leaf gene expression. In particular this platform can reliably detect genes expressed at very low levels to a much greater extent than the Affymetrix gene chip,24 and the coverage is 75−80% of the expected gene number of maize.

For all comparisons, a double loop design was used (Supplementary Fig. 1).26 In these experiments, samples were compared one to another in a daisy-chain fashion. These designs, combining loops with reference designs improved efficiency and robustness of the analysis by creating multiple links among samples; evaluations between samples not compared directly are computationally derived. 26 For all biological replicates, dye swap labeling was done, that is, for each quadruplicate, two replicates were labeled using Cy3 dye and two using Cy5 dye.

In all experiments, RNAi transgenic lines knockdown to *chc101* and *mbd101* genes, together with their non-transgenic WT siblings were used in families segregating 1:1. For *chc101* lines, there was a 7.7-fold decrease in transcript levels compared to WT plants, while for *mbd101* the decrease was 6.8-fold. Four-week-old maize plants were grown in greenhouse conditions without UV-B radiation. A matched set of plants was treated for 8 h under UV-B lamps that were covered by either a polyester plastic (PE) that absorbs UV-B but transmits UV-A and white light (control, no UV-B) or under a plastic sheet (CA) that transmits all UV-B (UV-B). Spectra are provided in Supplementary Fig. 2. The UV-B intensity used is about 3-fold higher than solar UV-B. Plants looked healthy without any visible phenotype immediately after the treatments (also see ref. 18).

Samples consisted of a pool of leaf pieces at the top of the canopy nearest the light source from multiple individuals, to reduce any plant to plant variability. For each treatment/genotype combination, four independent RNA samples were prepared, representing four biological replicates of the experiments. Determination of significant differential expression was undertaken with analysis of variance (ANOVA) style models. 24 First, transcript levels in the transgenic lines were compared to those in the B73 non-transgenic siblings, both under greenhouse control conditions and after 8h UV-B treatment. Second, within a genotype, control and UV-B treated samples were also compared. Transcripts showing statistically significant changes and 1.5-fold differences as described in Methods were analyzed further.

## Assessing transcript diversity in adult leaves

Of the 44 K probes printed in the array, about 26 K showed a median probe intensity level above background. When the transcriptomes of *chc101* and *mbd101* RNAi transgenic plants were compared to that of B73 non-transgenic siblings, nearly all of these transcripts were expressed to a similar level in all three genotypes. However, 7.5% of the transcripts (N = 2114) showed a significant change when *chc101* or *mbd101* knockdown plants were compared to WT siblings, combining totals from the normal growth regime in the absence of UV-B and the 8 h UV-B treatment. These data indicate that altering the steady-state level of putative chromatin protein can dramatically alter the transcriptome.

The Venn diagrams in Figure 1 provide more detail. Under control conditions in the absence of UV-B, there is a group of transcripts in the transgenic plants that show 1.5 higher levels than in B73 (numbers in bold in the diagram, 77 for *chc101* and 60 for *mbd101*; Fig. 1A). Prior qRT-PCR measurements established that in both of these RNAi knockdown lines, the target gene as well as several other chromatin-associated transcript types were down-regulated. 18 This led to the proposal that these and two other RNAi chromatin knockdown genotypes that shared this property, are all deficient in chromatin remodeling and its consequences, but with this more comprehensive data set, it is clear that each RNAi line examined has a distinctive profile. In this microarray experiment, we found only five transcripts, fewer than 10% of the up-regulated group, that are increased in both transgenic lines: a phototropic-responsive NPH3 family protein, a nitrite transporter, a PE-PGRS family protein, and two unknown function proteins (Supplementary Table 1). The NPH3 protein has a putative role in light signal transduction; therefore, it is possible that these chromatin proteins may regulate other light responses besides those elicited by UV-B.

Specifically in the *mbd101* plants, increased transcripts include some DNA and chromatin binding proteins such us a bromodomain-containing protein (BG836061), a zinc finger protein F35 (TC301590), a putative auxin-regulated protein (TC310355), and a DNA topoisomerase III (TC291312) (Supplementary Table 1). In *chc101* plants, different DNA binding proteins showed increase expression: an ETTIN-like auxin response factor (TC283518), a RAV-like B3 domain DNA binding protein-like (TC301326), a putative proliferating cell nuclear antigen (TC313452), an ethylene-insensitive-3-like protein (TC293252), and a homeodomain leucine-zipper protein Hox8 (TC298016). Many more transcripts exhibit lower expression in *chc101* and *mbd101* knockdown plants compared to B73 plants (underlined, 375 in *chc101* and 303 in *mbd101*, with 51 shared transcripts; Fig. 1A). Under control greenhouse conditions it appears that the CHC101 and MBD101 gene products are required for the transcriptional activity of many other genes. As with the up-regulated transcript set, most (~85%) of the differentially expressed transcripts were line-specific.

Collectively these results demonstrate that even under optimal growing conditions the RNAi lines have distinctive properties from the B73 inbred and from each other. Furthermore, summing the up- and down-regulated transcript types, 1.4% of the leaf transcriptome (N=363) is altered in *mbd101* and 1.7% (N=452) in the *chc101* knockdown line compared to WT

siblings. Therefore, these RNAi plants show substantially altered gene expression, likely reflecting the importance of the target genes in establishing chromatin configurations that are pre-requisite for expression of many genes.

### Differences in transcriptomes are increased by UV-B radiation

It is clear that UV-B modulates significantly the transcriptome of the transgenic lines when compared to the WT transcriptome. The *mbd101* line has 363 altered transcripts in the absence of UV-B, while 656 transcripts are changed after 8 h of UV-B irradiation. In *chc101* 452 mRNAs are differentially expressed in control conditions without UV-B and 769 when plants are exposed to UV-B (Fig. 1B). After UV-B exposure, the number of up-regulated genes in the *mbd101* RNAi line is noteworthy (618 increased versus 38 decreased). This suggests an involvement of UV-B in the de-repression of some epigenetically silenced genes, which may be kept repressed by MBD101 activity during the radiation treatment in the WT plants. In contrast, 143 transcripts are increased while many more are decreased (626) in the *chc101* mutants compared to the WT in the presence of UV-B; this supports the proposed role of CHC101 in transcriptional activation of diverse targets.

Among the transcripts designated as differentially regulated in one knockdown line, a few were expressed to the same extent under control and supplementary UV-B conditions (37 for *chc101* and 4 for *mbd101*, Supplementary Table 1). The two transgenic lines also share a small number of differentially regulated genes under control conditions (N=56, less than 10% of the total gene count Fig. 1A) and an even smaller number after UV-B (N=13, about 1% of the total, Fig. 1B). Therefore, although the plant phenotypes of UV-B hypersensitivity are similar, the transcriptome changes are primarily line-specific in the *mbd101* and *chc101* knockdown lines. Finally, it is interesting to note that there are 19 (less than 2% of the total differentially regulated transcripts) transcripts that show increased levels in UV-B irradiated *chc101* plants and also in *mbd101* plants under control greenhouse conditions compared to WT under the same light conditions (Fig. 1C). This could be explained if the down-regulated proteins perform the postulated roles of transcriptional activation by CHC101 and repression by MBD101.

### Within line comparisons of control to UV-B treatment conditions reinforce that distinct transcriptome responses occur in each line

When the control versus UV-B treatment transcriptomes of B73 plus the *chc101* and *mbd101* RNAi plants were analyzed, 1391 probes showed significant differential expression in response to the UV-B treatment in at least one maize line (Supplementary Table 2). This total is equivalent to 3.5% of the genes in the probe set and 5.4% of the leaf transcriptome demonstrating that heightened UV-B is a significant environmental challenge. Of these, 267 differentially expressed genes were modified by UV-B in the WT plants (128 increased, 139 decreased). Some of these genes were previously reported to be regulated by UV-B, confirming prior results, 18,20,21 and new genes are now designated as UV-B regulated in maize. In response to UV-B the transcriptomes of the transgenic lines are even more distinctive from each other and from B73 siblings than under control conditions. For the *chc101* RNAi line, there were fewer significant changes after UV-B (175 total, 72 increased and 103 decreased comparing control to UV-B transcriptomes within this line). In previous pilot studies by qRT-PCR, 18,19 decreased transcript abundance of a subset of these genes was found after UV-B treatment. In contrast, for the *mbd101* RNAi line, there were 897 transcripts that were up-regulated by UV-B but only 68 transcripts were down-regulated comparing the control to UV-B treatments. Therefore, the *mbd101* line has seven times more up-regulated and half as many down-regulated transcripts as the WT line.

Using qRT-PCR we previously reported about 2-fold increased levels of *chc101* and *mbd101* transcripts in B73 plants after the same UV-B treatment.18 Surprisingly, we did not

detect any significant increase in *mbd101* transcripts in this microarray study. For the *mbd101* probe (TC306104), the 60-mer has 96% similarity (56 of 60 identical) to *mbd120* (see http://www.chromdb.org); this second maize methyl binding domain protein will also hybridize with the 60-mer probe, hence cross-hybridization may mask differential expression. There is no probe for *chc101* on the arrays; there is a probe for *chc102*, which is 95% similar overall, however, within the 60-mer probe there are 14 mismatches sufficient to prevent cross-hybridization.

## Independent categorization of differential expression and functional classification

To continue the analysis, UV-B regulated genes were grouped according to similarity of expression patterns by self-organizing maps (SOMs) (Fig. 2, Supplementary Table 2). Fig. 2 shows 12 different patterns of transcript expression following UV-B in the three genotypes studied. The SOM analysis confirms that many transcripts are changed by UV-B in a genotype-dependent manner, reinforcing that both CHC101 and MBD101 proteins participate in gene expression regulation by UV-B in maize. For example, there are 119 genes that are only significantly increased by UV-B in the non transgenic B73 line (Fig. 2B). For down-regulated genes there is a similar observation: 128 transcripts are decreased by UV-B only in B73 (Fig. 2K). There are also genes that are only increased (823 in *mbd101* and 67 in *chc101*, Fig. 2G and J), or decreased (65 in *mbd101* and 93 in *chc101*, Fig. 2A and C) in the RNAi lines. This analysis confirms that both putative chromatin factors participate in transcription regulation by UV-B; importantly, deficiency in each factor alters the patterns of expression of many genes.

When the putative function of the gene products of the differentially regulated transcripts was analyzed, we observed that in the 1391 UV-B regulated genes, the major group (41%) corresponded to genes with unknown function as is typical for flowering plants; for clarity, the unknown category has been removed from this and subsequent pie chart representations in Fig. 3. The largest categories with ascribed function are transcripts for DNA/chromatin binding proteins (18.7%, Fig. 3A), general metabolism (16.4%), membrane proteins or proteins involved in transport (13.7%), receptors or signal transduction proteins (12.7%), stress or hormone responses (7.3%), protein synthesis (5.2%) and cytoskeleton (5.1%). Other groups each corresponded to less than a 5% of the total 819 transcripts with putative functions, for example those that encode for proteins that participate in protein degradation, chaperones, and RNA binding proteins (Fig. 3A). When the same classification was done for transcripts up-regulated exclusively in one line after UV-B treatment, we found that the main group again corresponded to DNA/chromatin binding proteins (17% for B73, 27.3% in *chc101* and 18.8% in *mbd101*). This list includes transcription factors, chromatin factors, and DNA repair proteins. This result suggests that most differences in UV-B responses in the WT and transgenic plants are mediated by transcriptional activation or repression of line-specific nuclear gene products that result in either tolerance (B73) or acute hypersensitivity (the RNAi lines).

In B73, cell wall-related proteins constitute the second largest regulated group (12.8%, Fig. 3B), however, no transcripts in this category were increased in *chc101*, and this category is only 4% in *mbd101*. It is possible that adding mass to the plant cell wall is an acclimation response to increase reflection of the radiation. Of known importance, some DNA repair proteins are increased only in B73; this is the case for a MutT-like protein (TC308231) and a DNA excision repair protein ERCC-1 (TC295292), which could participate in UV-B induced DNA damage repair by base or nucleotide excision repair, respectively. Their transcription is likely to be regulated by any or an earlier-expressed set of the up-regulated transcription factors in SOM B (Fig. 2). A second major category exclusive to B73 are a number of proteins categorized as stress and hormone response; they are 12.8% of the increased transcripts in B73. Their protein products (see Supplementary Table 2) can contribute to UV-B tolerance in B73. Also uniquely up-regulated in B73 after UV-B treatment are a suite of transcripts encoding

signal transduction or receptor proteins, mostly protein kinases (Fig. 3B); these are likely factors coordinating intracellular responses that induce tolerance. In contrast, the RNAi transgenic lines, show up-regulation of metabolic enzymes that are not usually induced by UV-B in B73 (Fig. 3B); this is the second most numerous category for these lines, after DNA/chromatin binding proteins. Four central pathways are represented: glycolysis, Krebs cycle, ATP synthesis, and lipid metabolism (Supplementary Table 2). During UV-B exposure, which is highly stressful to the RNAi plants, 18 increased capacities in these pathways provide energy from non-photosynthetic sources.

For uniquely down regulated proteins in B73, *chc101* or *mbd101* plants, DNA/chromatin binding proteins are the second largest group once again illustrating the impact UV-B has on this category of genes (Fig. 3C). Other highly represented categories include metabolic enzymes, which comprise 22.4% of uniquely down regulated transcripts in B73, 27.3% of the *chc101* decreased transcripts and 14.3% in *mbd101*. During UV-B acclimation, specific metabolic pathways are shut down or decreased – such as photosynthesis --20 and from this transcriptome profiling we can infer that many other metabolic pathways are modulated. Because the maize genome has small gene families encoding steps in central metabolism, different isozymes can be expressed in specific conditions; during responses to six different stress treatments, glycolysis and other energy generating systems were identified as key pathways with such novel isozyme expression. 24 Cells expend energy and reducing power to alleviate the oxidative and macromolecular damage stress caused by UV-B. In the UV-B hypersensitive transgenic plants there is a deficiency in the repression of genes encoding enzymes for these typically UV-B regulated pathways; the inability of the RNAi lines to redirect metabolism may result in increased cellular damage during UV-B exposure that is later scored as leaf curling and necrosis. Some pathways are also activated that are unchanged in the UV-B tolerant control line (Fig. 3C); mis-activation of pathways may be as deleterious to cell health as failing to properly differentially express specific isozymes in central metabolism.

## Expression of chromatin associated genes in UV-B regulation

Because functional classification of genes identified such a large fraction of UV-B regulated genes as DNA or chromatin interacting proteins, including transcription factors, we investigated them in more detail. For example, 12 DNA binding proteins are increased and 15 decreased by UV-B only in B73 (Fig. 2B and K, Table 1). Of the 12 increased DNA binding proteins, 2 are the predicted DNA repair proteins discussed previously (TC308231 and TC295292). As a check at the transcript accumulation level, qRT-PCR was done using primers specific to ERCC-1 (TC295292) cDNA from control and UV-B treated plants. Fig. 4 shows that while transcript levels for ERCC-1 are increased about 2.5-fold in B73 plants after 8h of UV-B irradiation; they are unchanged in *mbd101* or *chc101* transgenic plants, validating the quantification in the microarray analysis. All ten other DNA binding proteins up-regulated in B73 are predicted transcription factors (Table 1). Primers were designed for four proteins in this group [a Zinc finger protein F35 (TC301590), a SCARECROW-like protein (TC295581), a TA1 protein-like (CO453792), a DNA-binding protein RAV1-like (TC285041)]. All these putative transcription factors are induced by UV-B in B73 but are not changed (or increased but to a lesser extent) in the transgenic lines (Fig. 4). Thus, both MBD101 and CHC101 are necessary for induction of a subset of transcription factors by UV-B in maize, at least in the B73 genotype. These transcription factors possibly control the expression of some genes identified as differentially regulated in the transgenic lines. Modulation of transcription factor abundances may result in the very different transcriptome profiles and may define the largely independent transcript profiles for *mbd101* and *chc101* plants compared to each other and to non-transgenic siblings.

Additionally, there are several DNA binding proteins that are not induced by UV-B in WT plants but are induced by UV-B in the *chc101* or *mbd101* RNAi mutants. WRKY transcription factors 28 (TC300389) and 32 (TC293926) are up-regulated by UV-B only in *mbd101* plants; an ERF transcriptional factor 3 (TC305954), a DNA gyrase subunit (BI992346), and ABI5 (a bZIP protein, TC301287) show increased levels by UV-B in *chc101* plants (Fig. 4). Also, there are some transcription factors that are increased by UV-B in both RNAi lines. As quantified by qRT-PCR, a ZmMybst1 protein (TC312601) is increased about 2-fold after UV-B treatment in *chc101* and *mbd101* but is unchanged in WT B73 plants. Thus despite the likely differing roles of the two putative chromatin proteins and largely distinct transcriptome responses, their deficiency may elicit similar responses in particular cases, as we previously observed. 19 These results extend to UV-B down regulated transcription factors (Table 1). In conclusion, the microarray profiling on a sensitive platform containing most annotated maize genes has identified several dozen transcription factors that are likely to be responsible for successful acclimation in WT and whose mis-expression in the RNAi lines is predicted to lead to acute hypersensitivity. To our knowledge, none of the transcription factors identified in this work has previously been linked to UV-B responses in maize; however, they now clearly represent major candidates for the functional assessment of their roles in the hierarchy of UV-B responses and in the UV-B modulated transcriptional network.

## Discussion

We investigated the transcriptome of RNAi knockdown lines targeting two putative chromatin factors (a methyl-CpG-binding domain protein MBD101 and a chromatin remodeling complex protein CHC101) that exhibit identical phenotypic consequences of UV-B exposure. After *chc101* and *mbd101* plants were irradiated for 8 h with UV-B lamps, 4 week old plants showed increased downward arching of adult leaves; while after 4 daily doses of UV-B these transgenic lines and two expressing RNAi to other chromatin-associated genes showed visible leaf injury, including leaf necrosis, which progressively worsened during a one-week recovery without UV-B. 18 UV-B absorbing sunscreen pigments are a key factor in acclimation responses in WT plants, 20 the concentration of these molecules was lower in the transgenic plants compared to their non-transgenic siblings. 18 Finally, both *mbd101* and *chc101* RNAi transgenic lines had lower levels of transcripts for a number of other chromatin-associated proteins, suggesting that down-regulation of one putative chromatin protein caused a sweeping change in expression of this class of genes. Based on these common phenotypes, we hypothesized that the *mbd101* and *chc101* lines would have very similar transcriptome defects under control and UV-B illumination, compared to WT siblings.

What we demonstrated by transcriptome profiling is that these two RNAi lines exhibit substantially different transcriptome changes both compared to each other and to UV-B tolerant non-transgenic siblings under normal growth conditions. Nearly 3% (N=759) of the 26K transcripts present in WT leaves under control conditions without UV-B are modulated in one or both of the RNAi lines; 93% of these differentially regulated genes are line-specific (Fig. 1A). After 8 h of UV-B exposure 5.4% of the transcriptome (N=1412) is differentially regulated in the RNAi lines compared to WT and 99% of the transcriptome changes are line-specific. Therefore, despite the similarity in plant phenotypes and a small suite of shared responses, each RNAi line has a distinctive profile in the scope and individual genes differentially expressed.

*mbd101* encodes a putative methyl-CpG-binding domain (MBD) protein; many MBD proteins interact with DNA when it is methylated in cytosine bases. Methylation is a common epigenetic modification of DNA found in the genomes of most organisms. Methylation of cytosine is catalyzed by specific DNA methyltransferases, 27-29 which transfer a methyl group from the donor *S*-adenosyl-L-methionine to the 5 position of the pyrimidinic ring. Methylation on

cytosine is maintained by DNA methyltransferases when they occur at symmetrical contexts, i.e., CpG and CpNpG (where N is any nucleotide). 29 Cytosine methylation may affect gene expression in two ways: it can impede or recruit the binding of some transcription factors to their DNA recognition sequence, 30,31 and, by means of specific 5-methylcytosine binding proteins, it can induce nucleosome repositioning or the formation of repressive chromatin. 32,33 MBD proteins have recently been studied in plants, in particular in *A. thaliana* (reviewed in ref. 34). In Arabidopsis, there are 13 MBD genes, while maize has 14 based on sequence similarity. Out of the 13 members of the AtMBD family, 8 were found to bind methylated CpG sites; it is not clear what the roles for the other MBDs that do not bind methylated CpG sites are. There is no evidence that the orthologs of maize MBD101 bind to methylated DNA in Arabidopsis. Therefore, the role of MBD101 in maize is not clear. It has been proposed that monocot MBD proteins in particular have acquired functions other than binding to methylated CpG sites, such as binding to unmethylated DNA, 35 or binding to RNA, 36 and/or mediating protein–protein interactions. 37,38

In comparing transcripts under control and UV-B conditions within a line, the *mbd101* RNAi lines show many more line-specific transcript changes (897 up, 68 down) than either B73 or the *chc101* line (72 up, 103 down, Supplementary Table 2). Previously, we reported18 that the *mbd101* line expresses several transcripts more highly than WT controls after UV-B: a mismatch repair protein (AW4555671), a pre-rRNA processing protein RRP5 (AW424457), a NADPH-cytochrome P450 oxidoreductase (AW267179), and a histone acetyltransferase HAC101(AW056341). We also measured decreased levels of other transcripts when compared to WT, such as a histone acetyltransferase HD2 HDT104 (AI622604), an alcohol dehydrogenase (AW330922), a snRNP Sm protein F-like (AW330881), a histone acetyltransferase HAG101 (AW155759), and a chromatin assembly factor group C NFC102 (AW155846). 18,19 With the larger current data set, the significantly higher number of transcripts increased by UV-B in this line suggests that MBD101 has a major role in gene repression as do other MBD proteins 30,31 and that the RNAi knockdown lines lack sufficient activity to repress a large number of genes that are normally down-regulated during UV-B. We hypothesize that decreased levels of MBD101 could permit transcription factor binding to DNA recognition sequences, even if DNA is methylated, or it could relieve the formation of repressive chromatin.

On the other hand, CHC101 activity is implicated as crucial for transcriptional activation of acclimation genes after UV-B exposure. It is clear from this microarray profiling study that perturbation of CHC101 in maize has profound consequences under normal growth conditions in which nearly 2% of leaf transcripts are mis-regulated. There is an even larger effect after UV-B exposure in which 3% of transcripts are mis-regulated compared to WT siblings. These impacts are primarily a failure to express genes up to normal levels or to induce transcript abundance changes during UV-B. There are 143 transcripts that are increased while many more are decreased (626) in *chc101* mutants compared to the WT in the presence of UV-B. This suggests that a consequence of decreased CHC101 is a failure to trigger acclimation responses in a timely manner. *chc101* encodes a putative component of the SWI/SNF chromatin remodeling complex; the SWIB domain-containing protein. SWI/SNF chromatin-remodeling complexes mediate ATP-dependent alterations of DNA–histone contacts. SWI/SNF-like complexes studied in yeast, Drosophila, and mammals constitute at least nine subunits; the evolutionarily conserved core SWI/SNF subunits are essential and sufficient to remodel chromatin in vitro. 39,40 Mutations in genes encoding SWI/SNF subunits in yeast cause defects in mating-type switching and sucrose fermentation and affect the transcription of 5% of yeast genes. 41,42 In various mammalian SWI/SNF complexes, core subunits are combined with different regulatory subunits, including histone deacetylase and retinoblastoma tumor-suppressor Rb binding proteins (RbAP48). *A. thaliana* has four members of SWI/SNF ATPases, while rice (*Oryza sativa*) has three (http://www.chromdb.org/;43-45). Functional

overlap between individual members of this family; would allow assembly of specialized SWI/SNF complexes for various chromatin-based regulatory functions. 46 Our data demonstrate that decreased expression of one family member, maize *chc101*, impacts expression of many UV-B regulated genes.

Analysis of the 267 gene expression changes in the B73 control line after 8 h of UV-B exposure indicate that modulation of transcription factor and other chromatin/DNA binding proteins is a key response as this is the largest category of affected genes (Fig. 2). With further exploration of the newly identified transcription factors up-regulated by UV-B in WT plants, the hierarchy of responses to UV-B can be elucidated as well as the targets for these regulatory proteins. The largest category of differentially regulated transcript types was also DNA binding/chromatin in the two RNAi lines. These lines are mis-expressing (either up- or down-regulating) both transcription factors and chromatin associated proteins; the latter point was established in previous studies.18 Cell death and organismal death of seedlings are likely to be consequences of the combination of failure to properly up-regulate transcription factors required to activate acclimation pathways and the mis-activation or repression of other pathways that are unchanged in WT. Of immediate consequence during UV-B exposure, the RNAi lines fail to upregulate two genes encoding DNA repair proteins: a MutT-like protein (TC308231) and a putative DNA excision repair protein ERCC-1 (TC295292), which participate in DNA damage repair by base or nucleotide excision repair, respectively. We have determined that both *chc101* and *mbd101* RNAi plants have increased DNA damage during UV-B exposure and that repair takes longer than WT plants (Casati et al, unpublished); both of these phenotypes could reflect lower levels of DNA repair proteins.

UV-B elicits at least one additional DNA-level event: epigenetic reactivation of quiescent *Mu*-type maize transposons; 47 this reactivation is accompanied by decreased histone methylation around the ~215 bp terminal inverted repeats at the ends of *Mu* elements (Casati and Walbot, unpublished). Thus, it is possible that de-repression of genes is enhanced in the presence of UV-B, whether triggered by DNA repair unaccompanied by DNA methylation or other processes. In maize about 25% of C residues are methylated under normal conditions, 48 and it is not yet known, beyond the loss of DNA methylation at the termini of *Mu* transposons, if this epigenetic mark is modulated during UV-B acclimation at discrete sites throughout the genome.

Collectively these data greatly expand the list of UV-B responsive genes in a normal inbred line at one treatment dosage. Furthermore, we conclude that the RNAi knockdown lines are hypersensitive to UV-B for different reasons: in *mbd101* plants many genes are inappropriately expressed (ectopic activation) while in *chc101* plants too few normally UV-B responsive genes are properly activated. A major goal of future studies will be to determine the in vivo roles of MBD101 and CHC101 in maize.

## Methods

### Plant Material

Transgenic lines were deposited by the Plant Chromatin consortium at the Maize Genetics Stock Center (http://www.aces.uiuc.edu/maize-coop/). The transgenic lines are in a hybrid, mainly B73 background, and each contains an RNAi construct directed toward a specific target gene (for more information about the transgenic lines see http://www.chromdb.org/). For *chc101* plants, stock 3201−01 T-MCG3348.02 was used; for *mbd101* plants, stocks 3201−11 TMCG3818.11 and 3201−12 T-MCG3818.15 were used. For more information about the vectors used for transgenic plant construction, see http://www.chromdb.org/rnai/vector_info.html; and for information on the characteristics of the transgenic plants see Casati et al. 18,19. As non-transgenic controls, siblings with the same

genetic background but which lack the transgene construct encoding BASTA® herbicide resistance and an RNAi expression cassette were used. Lines heterozygous for the transgene (RNAi//-) were crossed by normal siblings to generate progeny families segregating 1:1 for the transgene; amalgamations from the different segregating families were used in some analyses. Segregation of the transgene was followed by BASTA® herbicide resistance test, presence of the transgene by PCR, and transcript levels by qRT-PCR.

### Radiation Treatments and Measurements

For all experiments, plants were germinated under supplemental visible lighting to 20% of summer noon radiation without UV-B in greenhouse conditions. After that, plants were illuminated with UV-B lamps using fixtures mounted 30 cm above the plants (Phillips, F40UVB 40 W and TL 20 W/12) for 8 h; leaf samples were collected immediately after the radiation treatment. The bulbs were covered with CA filters to exclude wavelengths lower than 280 nm. As a control, plants were exposed for the same period of time under the same lamps covered with PE that absorbs all wavelengths lower than 320 nm (no UV-B treatment). The output of the UV-B source was recorded using an Optronics 752 spectroradiometer (Optronics Laboratories, Orlando, Fl) equipped with a certified internal standard.

### RNA Isolation, Target cRNA Preparation and Array Hybridization

RNA and samples were prepared as described by Casati and Walbot 20 from a pool of top leaves from control or UV-B treatments. Target cRNA was prepared and labeled with either Cy3 or Cy5 dye (PerkinElmer, Boston, MA, USA) from 3 μg of total RNA using an Agilent Low RNA Input Fluorescent Linear Amplification Kit. Array hybridizations were carried out according to the manufacturer's instructions. For the experiments, Agilent Technologies microarrays were used, they contained 43,451 maize 60-mer probes synthesized in 4 subarrays per slide (4×44 version), control probes were detected with spike-in controls varying in concentration to permit validation of quantitative levels of gene expression in this design. Specifically, each array was hybridized with two samples, each of 0.825 μg labeled target cRNA, for 17 hours at 60°C. The samples were hybridized in a double loop design arrangement, as described by Kerr and Churchill (Supplementary Fig. 1). 25 Data were acquired with an Agilent G2565BA scanner. Hybridizations for all 12 comparisons were highly correlated as assessed from correlations between median signal intensities ($r^2 = 0.97$ for both dyes; data not shown) and between log2 ratios of the signals ($r^2 = 0.94$; data not shown). Oligonucleotide sequences, gene identities and both raw and normalized hybridization intensities for each probe can be downloaded from our array data deposited in the Gene Expression Omnibus database (http://www.ncbi.nlm.nih.gov/geo/) with accession number GSE 10400.

### Microarray Data Analysis

The reliability and reproducibility of analyses was ensured by the use of quadruplicates in each experiment, the normalization of all 12 arrays to the median probe intensity level with background subtracted, and the use of well accepted and freely available software packages. The slide images were processed with Feature Extraction v. 9.5 (Agilent), including normalization of the data. After filtering out the few saturated spots flagged by Feature Extraction, and for each slide, we first calculated thresholds for background hybridizations with the internal negative controls, as described previously. 24

All statistical analyses were performed using either the R package (http://www.r-project.org/) or Microsoft EXCEL (http://www.microsoft.com) as described in Fernandes et al. 24 After normalization each experiment was analyzed separately, using analysis of variance (ANOVA) style models, and the differentially expressed transcripts were selected based on an unadjusted *P* value of 0.05 and a log ratio cutoff of 0.58 and −0.58 (a 1.5-fold expression ratio). The final list comprised probes that were listed as significantly different

in at least three comparisons out of the total four comparisons. This list was annotated against transcript assemblies or ESTs from the TIGR wheat transcript assembly database (http://www.plantta.tigr.org/), using BLAST and filtering on a stringent e-value cutoff of 1e-05. For visualization, clustering of log 2 values of the expression ratios was performed using the "Cluster" program (Eisen Software, Lawrence Berkeley National Lab and the University of California at Berkeley, available from http://www.rana.lbl.gov/EisenSoftware.htm). To interpret the data, genes were grouped according to similarity of expression profiles with self-organizing maps or SOMs.

### Quantitative RT-PCR

Primers were designed using the Primer3 software (Rozen and Skaletsky, 2000) and are listed in Table 2. Five μg of total RNA from each genotype/treatment combination was used for cDNA synthesis using Superscript III reverse transcriptase (Invitrogen, Carlsbad, CA). Quantitative, real-time PCR (qRT-PCR) was carried out in a DNA Engine OPTICON2 (MJ Research a division of Bio-Rad, Hercules, CA) as described in Casati and Walbot. 21 Three replicates were performed for each sample plus template-free samples and other negative controls (reaction without reverse transcriptase). To normalize the data to the non-transgenic controls, primers for a thioredoxin-like transcript were used. To confirm the size of the PCR products, and to check that they corresponded to a unique and expected PCR product, the final PCR products were evaluated on a 2% agarose gel in comparison to size standards; thermal denaturation profiles were obtained from the OPTICON2 at the end of the PCR reactions to check that the product had the exptected $T_m$.

## Supplementary Material

Refer to Web version on PubMed Central for supplementary material.

## Acknowledgments

The project was supported by the NIH (R03 TW07487) funded by the Fogarty International Center. P. C. is a member of the Research Career of the Consejo Nacional de Investigaciones Científicas y Técnicas (CONICET) of Argentina. We thank Darren Morrow for help with the microarray hybridizations, John Fernandes for his assistance with the microarray data normalization and initial analysis and Lorena Falcone for helpful comments.

## Abbreviations

CA, cellulose acetate filter transmitting UV-B; PE, polyester plastic removing UV-B; CHC101, proposed chromatin remodeling complex protein of the SWI/SNF class; MBD101, protein related to methyl-CpG-binding domain protein; qRT-PCR, quantitative real-time polymerase chain reaction; SOM, self-organizing map; UV-B, ultraviolet-B radiation (280−320 nm); WT, wild-type.

## References

1. Pfluger J, Wagner D. Histone modifications and dynamic regulation of genome accessibility in plants. Curr Opin Plant Biol 2007;10:645–652. [PubMed: 17884714]
2. Eberharter A, Becker PB. Histone acetylation: A switch between repressive and permissive chromatin. Second in review on chromatin dynamics. EMBO Reports 2002;3:224–229. [PubMed: 11882541]
3. Vaillant I, Paszkowski J. Role of histone and DNA methylation in gene regulation. Curr Opin Plant Biol 2007;10:528–533. [PubMed: 17692561]
4. Britt AB. DNA damage and repair in plants. Annu Rev Plant Physiol Plant Mol Biol 1996;4:75–100. [PubMed: 15012283]

5. Gerhardt KE, Wilson MI, Greenberg BM. Tryptophan photolysis leads to a UVB-induced 66 kDa photoproduct of ribulose-1,5-bisphosphate carboxylase/oxygenase (Rubisco) in vitro and in vivo. Photochem Photobiol 1999;70:49–56.
6. Casati P, Walbot V. Crosslinking of ribosomal proteins to RNA in maize ribosomes by UV-B and its effects on translation. Plant Physiol 2004;136:3319–3332. [PubMed: 15466230]
7. Bergo E, Segalla A, Giacometti GM, Tarantino D, Soave C, Andreucci F, Barbato R. Role of visible light in the recovery of photosystem II structure and function from ultraviolet-B stress in higher plants. J Exp Bot 2003;54:1665–1673. [PubMed: 12754266]
8. Waterworth WM, Jiang Q, West CE, Nikaido M, Bray CM. Characterization of Arabidopsis photolyase enzymes and analysis of their role in protection from ultraviolet-B radiation. J Exp Bot 2002;53:1005–1015. [PubMed: 11971912]
9. Mazza CA, Boccalandro HE, Giordano CV, Battista D, Scopel AL, Ballaré CL. Functional significance and induction by solar radiation of ultraviolet-absorbing sunscreens in field-grown soybean crops. Plant Physiol 2000;122:117–125. [PubMed: 10631255]
10. Bieza K, Lois R. An *Arabidopsis* mutant tolerant to lethal ultraviolet-B levels shows constitutively elevated accumulation of flavonoids and other phenolics. Plant Physiol 2001;126:1105–1115. [PubMed: 11457961]
11. Brosche M, Strid A. Molecular events following perception of ultraviolet-B radiation by plants. Physiol Plant 2003;117:1–10.
12. Frohnmeyer H, Staiger D. Ultraviolet-B radiation-mediated responses in plants. Balancing damage and protection. Plant Physiol 2003;133:1420–1428. [PubMed: 14681524]
13. Ulm R, Nagy F. Signalling and gene regulation in response to ultraviolet light. Curr Opin Plant Biol 2005;8:477–82. [PubMed: 16039155]
14. Ulm R, Baumann A, Oravecz A, Mate Z, Adam E, Oakeley EJ, Schafer E, Nagy F. Genome-wide analysis of gene expression reveals function of the bZIP transcription factor HY5 in the UV-B response of Arabidopsis. Proc Natl Acad Sci USA 2004;101:1397–1402. [PubMed: 14739338]
15. Brown BA, Cloix C, Jiang GH, Kaiserli E, Herzyk P, Kliebenstein DJ, Jenkins GI. A UV-B-specific signaling component orchestrates plant UV protection. Proc Natl Acad Sci USA 2005;102:18225–18230. [PubMed: 16330762]
16. Madronich S, Mckenzie Rl, Caldwell M, Bjorn LO. Changes in ultraviolet-radiation reaching the earth's surface. AMBIO 1995;24:143–152.
17. Casati P, Walbot V. Differential accumulation of maysin and rhamnosylisorientin in leaves of high altitude landraces of maize after UV-B exposure. Plant Cell Environ 2005;28:788–799.
18. Casati P, Stapleton AE, Blum JE, Walbot V. Genome-wide analysis of high altitude maize and gene knockdown stocks implicates chromatin remodeling proteins in responses to UV-B. Plant J 2006;46:613–627. [PubMed: 16640598]
19. Casati P, Campi M, Chu F, Suzuki N, Maltby D, Guan S, Burlingame AL, Walbot V. Histone acetylation and chromatin remodeling are required for UV-B–dependent transcriptional activation of regulated genes in maize. Plant Cell 2008;20:827–842. [PubMed: 18398050]
20. Casati P, Walbot V. Gene expression profiling in response to ultraviolet radiation in maize genotypes with varying flavonoid content. Plant Physiol 2003;132:1739–1754. [PubMed: 12913132]
21. Casati P, Walbot V. Rapid transcriptome responses of maize to UV-B in irradiated and shielded tissues. Genome Biol 2004b;5:R16. [PubMed: 15003119]
22. Kirst M, Caldo R, Casati P, Tanimoto G, Walbot V, Wise RP, Buckler ES. Genetic diversity contribution to errors in short oligonucleotide microarray analysis. Plant Biotec J 2006;4:489–498.
23. Ma J, Morrow DJ, Fernandes J, Walbot V. Comparative profiling of the sense and antisense transcriptome of maize lines. Genome Biology 2006;7:R22. [PubMed: 16542496]
24. Fernandes J, Morrow DJ, Casati P, Walbot V. Distinctive transcriptome responses to adverse environmental conditions in Zea mays L. Plant Biotech J. 2008in press
25. Sawers RJH, Liu P, Anufrikova K, Gene JTG, Brutnell TP. A multi-treatment experimental system to examine photosynthetic differentiation in the maize leaf. BMC Genomics 2007;8article 12
26. Kerr KM, Churchill GA. Statistical design and the analysis of gene expression microarray data. Genetical Research 2001;77:123–128. [PubMed: 11355567]

27. Hermann A, Gowher H, Jeltsch A. Biochemistry and biology of mammalian DNA methyltransferases. Cell Mol Life Sci 2004;61:2571–2587. [PubMed: 15526163]
28. Finnegan EJ, Kovac KA. Plant DNA methyltransferases. Plant Mol Biol 2000;43:189–201. [PubMed: 10999404]
29. Wada Y. Physiological functions of plant DNA methyltransferases. Plant Biotech 2005;22:71–80.
30. Inamdar NM, Ehrlich KC, Ehrlich M. CpG methylation inhibits binding of several sequence-specific DNA-binding proteins from pea, wheat, soybean and cauliflower. Plant Mol Biol 1991;17:111–123. [PubMed: 1831056]
31. Watt F, Molloy PL. Cytosine methylation prevents binding to DNA of a HeLa cell transcription factor required for optimal expression of the adenovirus major late promoter. Genes Dev 1988;2:1136–1143. [PubMed: 3192075]
32. Bird AP, Wolffe AP. Methylation-induced repression—Belts, braces, and chromatin. Cell 1999;99:451–454. [PubMed: 10589672]
33. Klose RJ, Bird AP. Genomic DNA methylation: the mark and its mediators. Trends Biochem Sci 2006;31:89–97. [PubMed: 16403636]
34. Grafi G, Zemach A, Pitto L. Methyl-CpG-binding domain (MBD) proteins in plants. Bioch Biophys Acta 2007;1769:287–294.
35. Scebba F, Bernacchia G, De Bastiani M, Evangelista M, Cantoni RM, Cella R, Locci MT, Pitto L. Arabidopsis MBD proteins show different binding specificities and nuclear localization. Plant Mol Biol 2003;53:755–771.
36. Jeffery L, Nakielny S. Components of the DNA methylation system of chromatin control are RNA-binding proteins. J Biol Chem 2004;279:49479–49487. [PubMed: 15342650]
37. Zemach A, Li Y, Wayburn B, Ben-Meir H, Kiss V, Avivi Y, Kalchenko V, Jacobsen SE, Grafi G. DDM1 binds Arabidopsis methyl-CpG binding domain proteins and affects their subnuclear localization. Plant Cell 2005;17:1549–1558. [PubMed: 15805479]
38. Saito M, Ishikawa F. The mCpG-binding domain of human MBD3 does not bind to mCpG but interacts with NuRD/Mi2 components HDAC1 and MTA2. J Biol Chem 2002;277:35434–35439. [PubMed: 12124384]
39. Phelan ML, Sif S, Narlikar GJ, Kingston RE. Reconstitution of a core chromatin remodeling complex from SWI/SNF subunits. Mol Cell 1999;3:247–253. [PubMed: 10078207]
40. Sudarsanam P, Winston F. The Swi/Snf family of nucleosome-remodeling complexes and transcriptional control. Trends Genet 2000;16:345–351. [PubMed: 10904263]
41. Cairns BR, Lorch Y, Li Y, Zhang M, Lacomis L, Erdjument-Bromage H, Tempst P, Du J, Laurent B, Kornberg RD. RSC, an essential, abundant chromatin-remodeling complex. Cell 1996;87:1249–1260. [PubMed: 8980231]
42. Ng HH, Robert F, Young RA, Struhl K. Genome-wide location and regulated recruitment of the RSC nucleosome remodeling complex. Genes Dev 2002;16:806–819. [PubMed: 11937489]
43. Flaus A, Martin DM, Barton GJ, Owen-Hughes T. Identification of multiple distinct Snf2 subfamilies with conserved structural motifs. Nucleic Acids Res 2006;34:2887–2905. [PubMed: 16738128]
44. Su Y, Kwon CS, Bezhani S, Huvermann B, Chen C, Peragine A, Kennedy JF, Wagner D. The N-terminal ATPase AT hook-containing region of the Arabidopsis chromatin-remodeling protein SPLAYED is sufficient for biological activity. Plant J 2006;46:685–699. [PubMed: 16640604]
45. Bezhani S, Winter C, Hershman S, Wagner JD, Kennedy JF, Kwon CS, Pfluger J, Su Y, Wagner D. Unique, shared, and redundant roles for the Arabidopsis SWI/SNF chromatin remodeling ATPases BRAHMA and SPLAYED. Plant Cell 2007;19:403–416. [PubMed: 17293567]
46. Sarnowski TJ, Swiezewski S, Pawlikowska K, Kaczanowski S, Jerzmanowski A. AtSWI3B, an Arabidopsis homolog of SWI3, a core subunit of yeast Swi/Snf chromatin remodeling complex, interacts with FCA, a regulator of flowering time. Nucleic Acids Res 2002;30:3412–3421. [PubMed: 12140326]
47. Walbot V. UV-B damage amplified by transposons in maize . Nature 1999;397:398–399. [PubMed: 9989403]
48. Hake S, Walbot V. The genome of *Zea mays*, its organization and homology to related grasses. Chromosoma 1980;79:251–270.

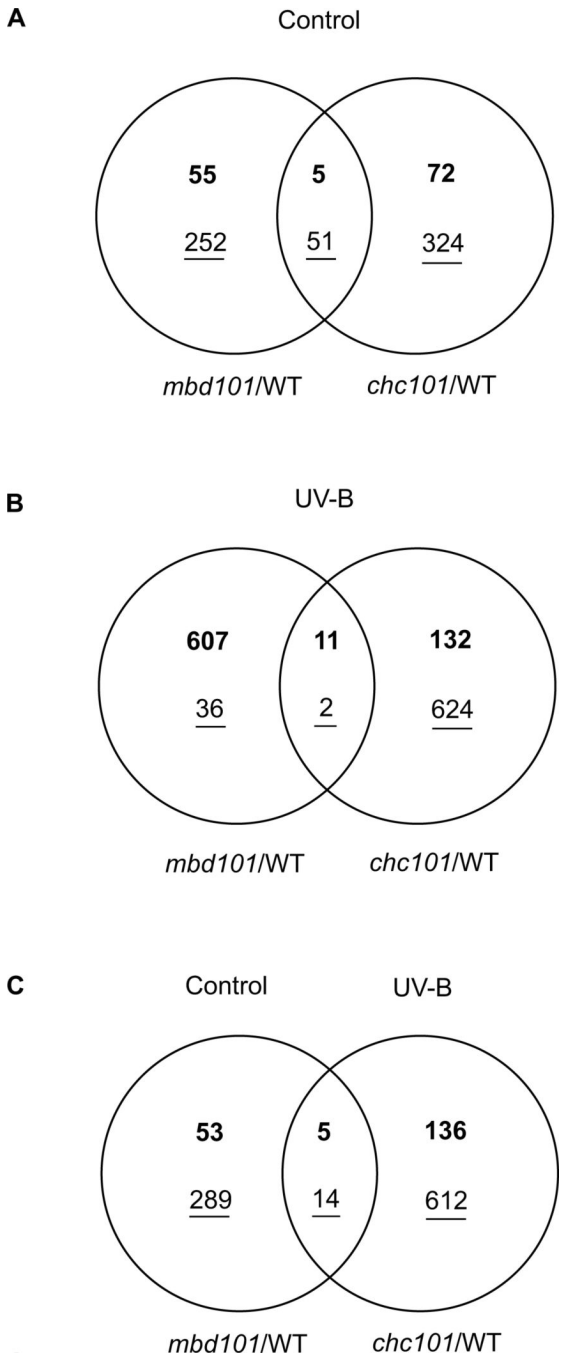


**Figure 1.**

Venn diagrams of comparisons between *mbd101* and *chc101* RNAi transgenic plants and B73 non transgenic siblings. Up-regulated genes are in bold, down-regulated genes are underlined. Sets of genes were selected using the criteria described in Methods. (A) Intersection of genes differentially expressed in *mbd101* and *chc101* RNAi lines in comparison to WT in greenhouse control conditions without UV-B. (B) Intersection of genes differentially expressed in *mbd101* and *chc101* RNAi lines in comparison to WT after 8 h of UV-B exposure. (C) Intersection of genes differentially expressed in *mbd101* RNAi plants in greenhouse control conditions without UV-B and *chc101* RNAi plants after 8 h of UV-B exposure; each RNAi line was compared to WT under the same light conditions.

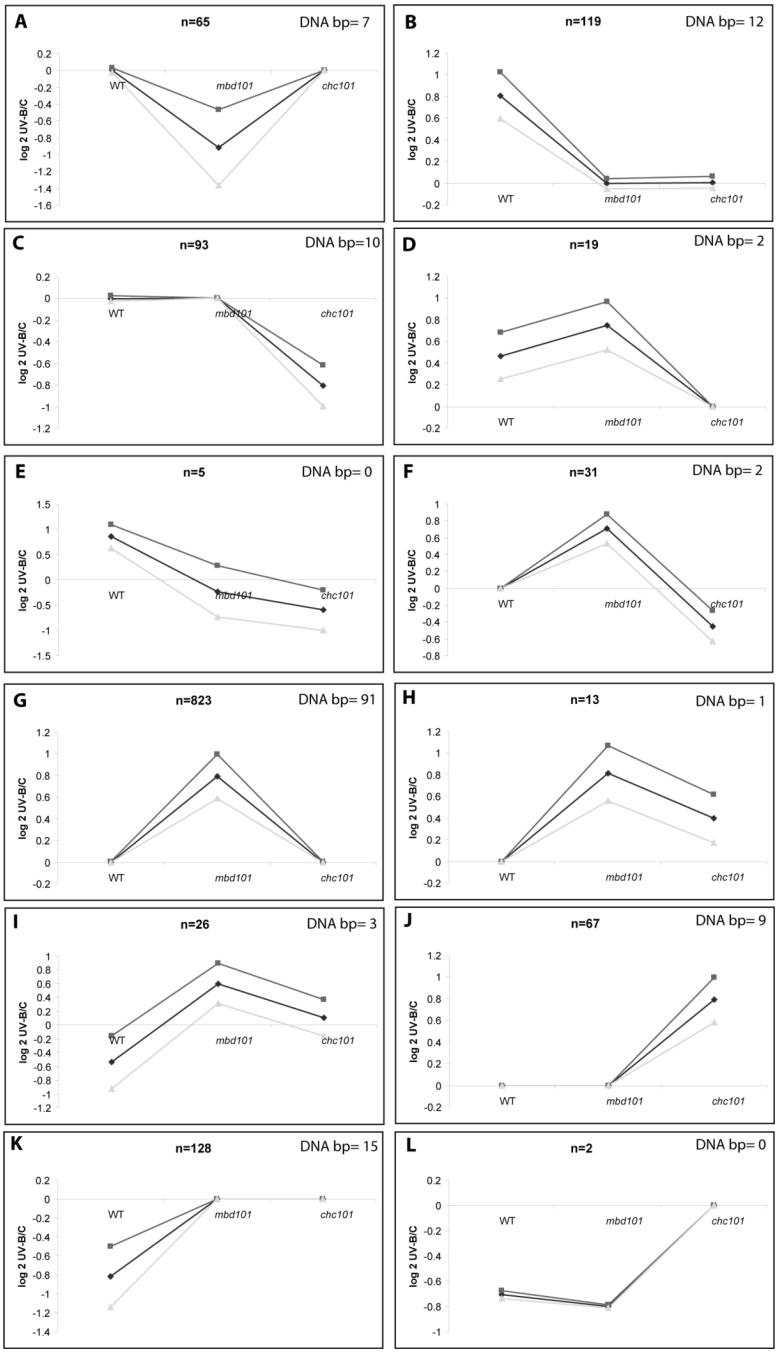


**Figure 2.**

Self-organizing map clusters of expression profiles from WT, *mbd101* and *chc101* RNAi plants after 8h of UV-B exposure. RNA samples from the lines not exposed to UV-B were used as the references. Each graph displays the mean pattern of expression of the ESTs in the cluster in black and the standard deviation of average expression (upper and lower gray lines). The number of probes in each cluster is at the upper center of each SOM, and the number of putative DNA binding proteins (bp) in each group is in the upper right of each SOM. The y axis represents log 2 of gene expression ratios.

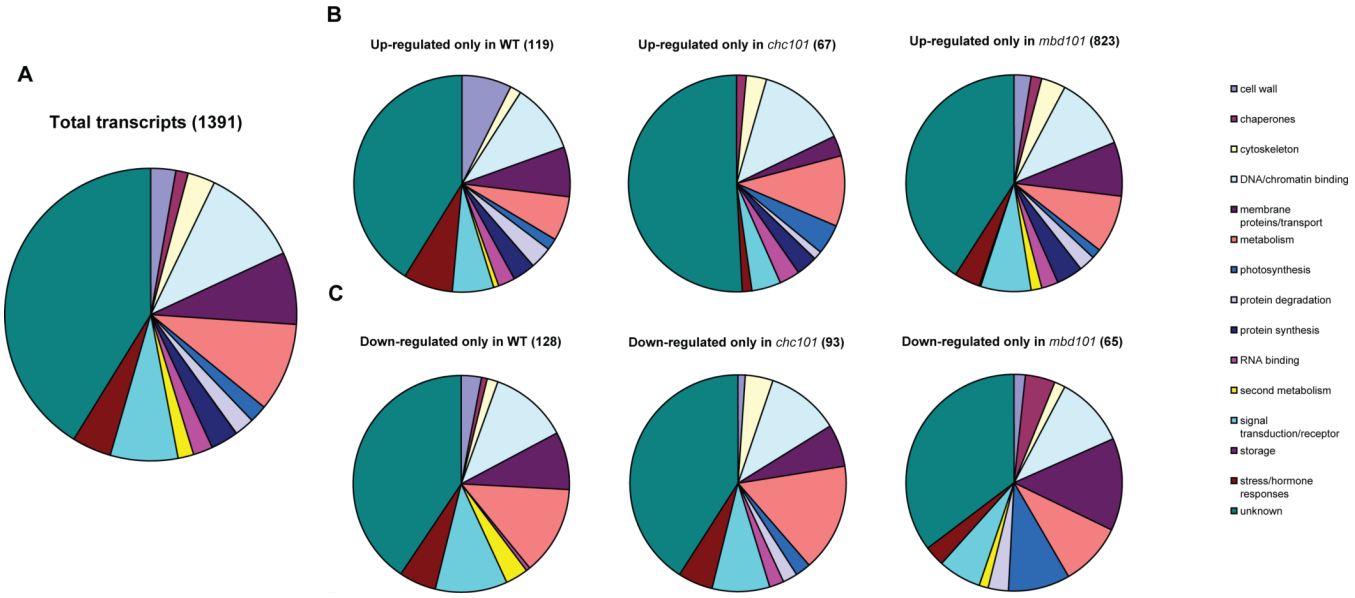


**Figure 3.**

Classification of UV-B regulated genes identified by microarrays based on their putative function. Classification was done for the total UV-B regulated transcripts in all lines (A), for up-regulated transcripts in each line (WT, *mbd101* and *chc101*, B), and for down regulated transcripts in each line (C). Transcripts with ratios at least 1.5-fold increased or decreased after the UV-B treatments were included in the diagrams.

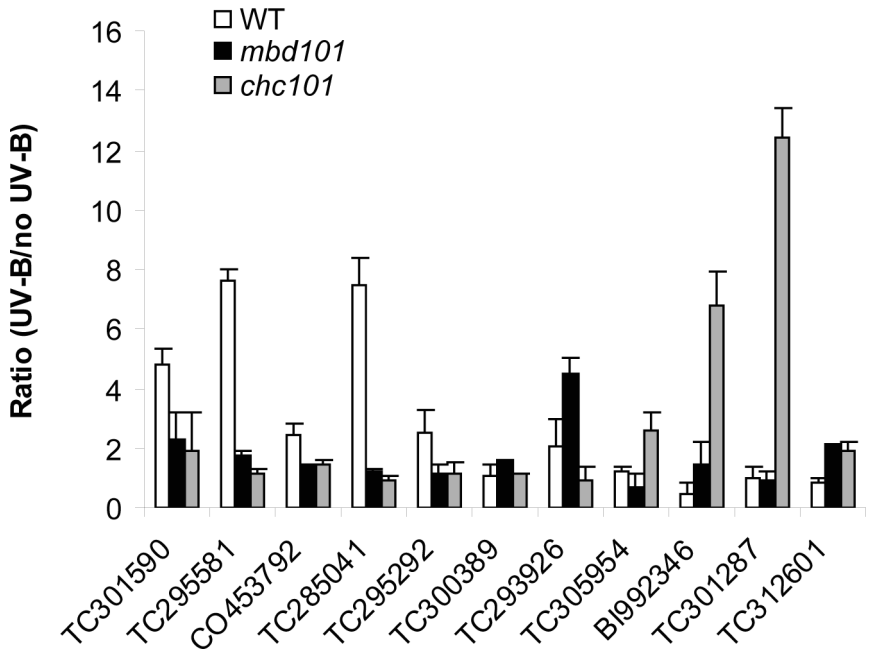


**Figure 4.**

Real-time qRT-PCR analysis to study the UV-B induction of gene expression in WT, *mbd101* and *chc101* RNAi plants of various DNA and chromatin binding proteins. 50 ng of cDNA after reverse transcription of RNA from WT (white), *mbd101* (black) and *chc101* (gray) plants after 8 h of UV-B and no UV-B treatments were used for Real-time PCR experiments. Experiments were done at least in triplicate with each sample and at least three independent RNA preparations (from experimental replicate pools of leaves) were employed. Error bars are standard errors.

**Table 1**

List of chromatin interacting proteins that are regulated by UV-B in B73 and/or *mbd101* and *chc101* RNAi lines clustered by SOM

| Group | Gene Name-Description | $log_2$ B73 (UV-B/C) | $log_2$*mbd101* (UV-B/C) | $log_2$*chc101* (UV-B/C) |
|---|---|---|---|---|
| A | TC290207 DNA binding protein-like | N.S. | −1.24 | N.S. |
| A | TC291296 Transcription factor Hap5a-like protein | N.S. | −1.05 | N.S. |
| A | DN211928 weakly similar to MOUSE Homeobox protein SIX3 | N.S. | −0.93 | N.S. |
| A | TC313175 hHAP3-like transcriptional-activator | N.S. | −0.91 | N.S. |
| A | TC313174 HAP3-like transcriptional-activator | N.S. | −0.72 | N.S. |
| A | BG316945 similar to polyprotein with nucleic acid binding site | N.S. | −0.78 | N.S. |
| A | TC298005 similar to Homeodomain leucine zipper protein 16 | N.S. | −0.68 | N.S. |
| B | TC301590 similar to Zinc finger protein F35 | 0.68 | **−0.40** | N.S. |
| B | DR814435 Zinc finger (C3HC4-type RING finger) protein-like | 0.59 | N.S. | N.S. |
| B | TC306513 similar to IAA1 protein | 0.58 | N.S. | N.S. |
| B | DN220462 similar to protamine P1 | 0.58 | N.S. | N.S. |
| B | DR829384 similar to Homeobox protein ARX | 0.60 | N.S. | N.S. |
| B | TC295581 SCARECROW-like protein | 0.60 | N.S. | N.S. |
| B | TC285041 DNA-binding protein RAV1-like | 0.98 | N.S. | N.S. |
| B | TC308231 MutT-like protein | 0.87 | N.S. | N.S. |
| B | CO453792TA1 protein-like | 1.09 | N.S. | N.S. |
| B | TC279435 Zinc finger protein | 0.82 | N.S. | N.S. |
| B | CO446587 homologue to IAA17:AXR3−1 protein | 0.69 | N.S. | N.S. |
| B | TC295292 DNA excision repair protein ERCC-1 | 0.81 | N.S. | N.S. |
| C | DT948508 Zinc finger protein-like | N.S. | N.S. | −0.74 |
| C | TC291028 SET domain protein SDG117 | N.S. | N.S. | −0.59 |
| C | DN219469 H6 homeodomain protein | N.S. | N.S. | −0.64 |
| C | TC288318 similar to DRE binding factor 1 | N.S. | N.S. | −1.00 |
| C | CO463653 WRKY transcription factor 6 | N.S. | N.S. | −0.97 |
| C | DT938212 zinc finger (HIT type) family protein | N.S. | N.S. | −1.02 |
| C | BM378658 similar to FRUITFULL-like MADS-box | N.S. | N.S. | −1.04 |
| C | TC281657 Basic helix-loop-helix SPATULA-like protein | N.S. | N.S. | −0.81 |
| C | TC295287 Bell-like homeodomain protein 4 | N.S. | N.S. | −0.83 |
| D | TC279425 4DNA-directed RNA polymerase beta chain | **0.32** | 0.89 | N.S. |
| D | TC313375 similar to En:Spm-like transposon protein | **0.43** | 0.62 | N.S. |
| F | TC305295 Exonuclease | N.S. | 0.88 | **−0.30** |
| F | TC303699 similar to FLK | N.S. | **0.48** | −0.71 |
| G | CV985340 Chromatin remodeling protein-like | N.S. | 0.74 | N.S. |
| G | TC283496 similar toprotamine P1 | N.S. | 0.78 | N.S. |
| G | TC303774 WRKY20 | N.S. | 0.79 | N.S. |
| G | TC291432 Leucine zipper protein-like | N.S. | 0.83 | N.S. |
| G | TC283259 PHD-finger domain protein | N.S. | 0.79 | N.S. |
| G | TC296661AREB-like protein | N.S. | 0.79 | N.S. |
| G | TC304824 Leucine zipper factor-like | N.S. | 0.84 | N.S. |
| G | TC281975 DEAD:DEAH box helicase domain containing protein | N.S. | 0.82 | N.S. |
| G | TC301947 Topoisomerase 6 subunit A | N.S. | 0.80 | N.S. |
| G | TC294271 Paxneb protein-like | N.S. | 0.83 | N.S. |
| G | DR800093 Transcription factor HBP-1a | N.S. | 0.83 | N.S. |
| G | TC283685 SNF2 domain-protein: helicase domain-protein: RING finger domain-protein | N.S. | 0.81 | N.S. |
| G | TC283727 Trad-like protein | N.S. | 0.76 | N.S. |
| G | TC312132 T7-like RNA polymerase | N.S. | 0.75 | N.S. |
| G | TC298228 similar to P18 | N.S. | 0.71 | N.S. |

| Group | Gene Name-Description | $log_2$ B73 (UV-B/C) | $log_2$*mbd101* (UV-B/C) | $log_2$*chc101* (UV-B/C) |
|---|---|---|---|---|
| G | TC282626 SWIRM domain-protein: DNA-binding protein | N.S. | 0.71 | N.S. |
| G | CO461684 DNA-binding protein | N.S. | 0.72 | N.S. |
| G | TC305932 Histone H1-like protein | N.S. | 0.72 | N.S. |
| G | CO523711 Transposase | N.S. | 0.71 | N.S. |
| G | DR804579 Zinc finger transcription factor ZF1 | N.S. | 0.71 | N.S. |
| G | TC300472 Transcription factor-like | N.S. | 0.75 | N.S. |
| G | TC302614 similar to MAR binding filament-like protein 1 | N.S. | 0.73 | N.S. |
| G | TC313735 Transcription factor Pti6-like | N.S. | 0.73 | N.S. |
| G | TC305491 zinc-binding family protein | N.S. | 0.98 | N.S. |
| G | TC297208 similar to MAZ | N.S. | 1.03 | N.S. |
| G | TC299847 similar to Growth-regulating factor 1 | N.S. | 1.01 | N.S. |
| G | TC301841 auxin-induced protein IAA18 | N.S. | 1.10 | N.S. |
| G | TC289906 Helix-turn-helix motif protein | N.S. | 1.32 | N.S. |
| G | TC292168 zinc finger (C3HC4-type RING finger) family protein | N.S. | 1.30 | N.S. |
| G | CF054233 similar to SPAC3G6.11 protein | N.S. | 1.50 | N.S. |
| G | TC300389 WRKY transcription factor 28 | N.S. | 1.53 | N.S. |
| G | TC293926 Transcription factor WRKY32 | N.S. | 1.12 | N.S. |
| G | TC296860 Ring-H2 zinc finger protein-like | N.S. | 1.11 | N.S. |
| G | TC301840 auxin-induced protein IAA18 | N.S. | 0.87 | N.S. |
| G | TC296531 SET domain-containing protein-like | N.S. | 0.90 | N.S. |
| G | TC292560 Histone H2B | N.S. | 0.89 | N.S. |
| G | TC293716 Remorin-like protein | N.S. | 0.86 | N.S. |
| G | TC295702 DNA-binding protein-like | N.S. | 0.85 | N.S. |
| G | TC283131 DNA-directed RNA polymerase family protein | N.S. | 0.85 | N.S. |
| G | TC313325 SCARECROW-like protein | N.S. | 0.86 | N.S. |
| G | TC309145 DNA binding protein-like | N.S. | 0.94 | N.S. |
| G | TC305464 myb family transcription factor | N.S. | 0.94 | N.S. |
| G | DT645737 DNA ligase-like | N.S. | 0.93 | N.S. |
| G | TC282596 cell death suppressor protein IIs1 | N.S. | 0.90 | N.S. |
| G | TC291216 similar to NAC domain protein NAC6 | N.S. | 0.92 | N.S. |
| G | TC299450 CAAT-box DNA binding protein subunit B (NF-YB) | N.S. | 0.62 | N.S. |
| G | TC301882 OSE2-like protein | N.S. | 0.61 | N.S. |
| G | TC288248 Origin recognition complex subunit 1 | N.S. | 0.62 | N.S. |
| G | TC313297 zinc finger (DHHC type) family protein | N.S. | 0.61 | N.S. |
| G | TC285381 DNA primase:helicase-like | N.S. | 0.61 | N.S. |
| G | TC307117 similar to Forkhead box protein D1 | N.S. | 0.63 | N.S. |
| G | TC282357 SET domain-containing protein SET102 | N.S. | 0.63 | N.S. |
| G | TC300575 Anti-silencing protein-like | N.S. | 0.62 | N.S. |
| G | TC294051 Transcription initiation factor IID subunit A-like protein | N.S. | 0.62 | N.S. |
| G | TC313065 OCL4 protein | N.S. | 0.63 | N.S. |
| G | TC284136 zinc finger protein-like | N.S. | 0.59 | N.S. |
| G | TC280091 Histone H2B.3 | N.S. | 0.59 | N.S. |
| G | TC302259 RING finger-like protein | N.S. | 0.59 | N.S. |
| G | BM078439 Response regulator 8 | N.S. | 0.58 | N.S. |
| G | TC293837 Probable CCAAT-binding transcription factor subunit HAP3B | N.S. | 0.58 | N.S. |
| G | CO455022 Transcription factor PCF8-like | N.S. | 0.59 | N.S. |
| G | DN230806 Transcriptional activator-like | N.S. | 0.60 | N.S. |
| G | TC282611 Nucleolar complex protein 2 homolog | N.S. | 0.60 | N.S. |
| G | TC289246 similar to DNA-binding Vsf-1 protein | N.S. | 0.63 | N.S. |
| G | TC301785 WRKY transcription factor 64-like protein | N.S. | 0.68 | N.S. |
| G | TC307302 Zinc finger (C3HC4-type RING finger) protein family-like | N.S. | 0.68 | N.S. |
| G | TC310357 similar to Aux:IAA protein | N.S. | 0.68 | N.S. |
| G | CO453237 homologue to Dof28 | N.S. | 0.67 | N.S. |

| Group | Gene Name-Description | $log_2$ B73 (UV-B/C) | $log_2$*mbd101* (UV-B/C) | $log_2$*chc101* (UV-B/C) |
|---|---|---|---|---|
| G | TC289954 zinc finger (C3HC4-type RING finger) family protein | N.S. | 0.69 | N.S. |
| G | TC284537 similar to zinc finger (C3HC4-type RING finger) protein | N.S. | 0.70 | N.S. |
| G | BM417644 similar to zinc finger (C3HC4-type RING finger) protein | N.S. | 0.70 | N.S. |
| G | TC283655 similar to MADS20 | N.S. | 0.70 | N.S. |
| G | BG836240 histone H1 | N.S. | 0.70 | N.S. |
| G | CF011836 H2A protein | N.S. | 0.69 | N.S. |
| G | TC294256 XIAP associated factor-1-like protein | N.S. | 0.64 | N.S. |
| G | TC290573 zinc finger (DHHC type) family protein | N.S. | 0.65 | N.S. |
| G | TC301974 similar to transcription factor S-II (TFIIS) domain-protein | N.S. | 0.65 | N.S. |
| G | TC304105 Zinc finger-like | N.S. | 0.65 | N.S. |
| G | TC294747 similar to Heat shock transcription factor 34 | N.S. | 0.64 | N.S. |
| G | TC303507 similar to Transducin:WD-40 repeat protein | N.S. | 0.64 | N.S. |
| G | TC284292 similar to transducin family protein: WD-40 repeat protein | N.S. | 0.64 | N.S. |
| G | TC294204 WD-40 repeat protein | N.S. | 0.64 | N.S. |
| G | TC282978 transducin family protein:WD-40 repeat protein | N.S. | 0.64 | N.S. |
| G | TC303579 WD-40 repeat protein-like | N.S. | 0.65 | N.S. |
| H | TC312601 ZmMybst1 | N.S. | 0.74 | 0.49 |
| I | TC299406 MutT domain protein-like | **−0.51** | 0.66 | N.S. |
| I | TC303578 Zinc finger-like | **−0.31** | 0.68 | N.S. |
| I | TC295265 exonuclease family protein | −0.98 | **0.40** | N.S. |
| J | TC307710 MADS-box protein RMADS220 | N.S. | N.S. | 0.94 |
| J | TC312727 DNA topoisomerase family protein | N.S. | N.S. | 0.78 |
| J | TC305954 BTH-induced ERF transcriptional factor 3 | N.S. | N.S. | 1.48 |
| J | TC301287 similar to Abscisic acid insensitive 5 (ABI5) (BZIP protein) | N.S. | N.S. | 1.12 |
| J | BI992346 DNA gyrase subunit B | N.S. | N.S. | 1.16 |
| J | TC307568 similar to heat shock factor RHSF5 | N.S. | N.S. | 1.02 |
| J | TC306750 N-acetyltransferase and Transcription factor-like protein | N.S. | N.S. | 0.72 |
| J | TC302820 MLH1 protein | N.S. | N.S. | 0.72 |
| J | TC296589 transducin family protein:WD-40 repeat family protein | N.S. | N.S. | 0.60 |
| K | TC282819 transducin family protein:WD-40 repeat family protein | −1.74 | N.S. | N.S. |
| K | TC311542 Transducin:WD-40 repeat protein-like | −3.36 | N.S. | N.S. |
| K | CF635962 DNA mismatch repair protein-like | −0.61 | N.S. | N.S. |
| K | TC307445 barren family protein | −0.63 | N.S. | N.S. |
| K | TC283503 zinc finger (B-box type) family protein | −0.69 | N.S. | N.S. |
| K | TC289797 HD2 type histone deacetylase HDA106 | −0.59 | N.S. | N.S. |
| K | CF273340 E2F protein | −0.62 | N.S. | N.S. |
| K | CD442931 Bzip transcription factor-like | −0.85 | N.S. | N.S. |
| K | TC301692 Flowering-time protein isoform alpha | −0.80 | N.S. | N.S. |
| K | CO445451 DNA POLYMERASE EPSILON | −0.79 | N.S. | N.S. |
| K | TC283529 DNA ligase | −0.95 | N.S. | N.S. |
| K | TC280485 LIM transcription factor homolog | −0.92 | N.S. | N.S. |
| K | AW061730 similar to KEAP1 | −0.71 | N.S. | N.S. |
| K | TC292191 homologue to NAC protein | −0.71 | N.S. | N.S. |
| K | TC284057 AP2 domain-containing protein AP29 | −0.77 | N.S. | N.S. |

**Table 2**

Primers used for qRT-PCR

| Transcript type | Accession number | Primer orientation | Primer sequence (5′ to 3′) |
|---|---|---|---|
| Zinc finger protein F35 | TC301590 | forward | TCAGCTTCTGGTGCTGGT |
| | | reverse | CGCTCTTCTGCAGCAACT |
| SCARECROW-like protein | TC295581 | forward | TCCTACAACGCACCCTTC |
| | | reverse | CGTTGATTGCCTCTCGAC |
| TA1 protein-like, partial (8%) | CO453792 | forward | TGCACGATGTGAAGCAAC |
| | | reverse | ATTATTTCGGCGGTGGAT |
| DNA-binding protein RAV1-like | TC285041 | forward | AAGCGAAGCAAGCATGAG |
| | | reverse | CCGTGGCAAACAAGAGAG |
| WRKY transcription factor 28 | TC300389 | forward | ATGCCTGGATTGCTGAAG |
| | | reverse | TTCACCCGGAGAGATTTG |
| WRKY transcription factor 32 | TC293926 | forward | CCTCTCGAGTGCTTTGGA |
| | | reverse | AAAAGCCCTGTTGGCTTC |
| ZmMybst1 | TC312601 | forward | TCCTTTCTGGCCAAATCA |
| | | reverse | GACACCGTTTCCTGACCA |
| DNA excision repair protein ERCC-1 | TC295292 | forward | TCTTTTGGGTCGCTCTCA |
| | | reverse | GAAGGTTGGCCTTTTGCT |
| BTH-induced ERF transcriptional factor 3 | TC305954 | forward | CACCCACAGCTCCAACAT |
| | | reverse | GGGCTTAGGCTCCTTTCA |
| DNA gyrase subunit B | BI992346 | forward | TCAATCCTTGCCTCCAGA |
| | | reverse | AGCAGCGAAGTGTGTGGT |
| Abscisic acid insensitive 5 | TC301287 | forward | GGCCAGGTGTTTTCCTCT |
| | | reverse | TCTCCAGCTCGTTGGTGT |
| Thioredoxin-like gene | AW927774 | forward | GGACCAGAAGATTGCAGAAG |
| | | reverse | CAGCATAGACAGGAGCAATG |

[a] Primers specifically designed to detected decreased transcript accumulation mediated by RNAi transformation